Terrace - Alluvial Fan Chronology based on ^{36}Cl buildup dating at the Organ Pipe Cactus National Monument, Arizona

by

Susan Hoines

Submitted in partial fulfillment of the requirements for the degree of Master of Science in Hydrology

New Mexico Institute of Mining and Technology

Socorro, New Mexico

Summer, 1993

Abstract

Simpson (1991) distinguished six geomorphic surfaces on the piedmont west of the Ajo Mountains in Organ Pipe Cactus National Monument based on their soil morphology and chemistry, topographic position, relief, surface morphology, stone pavement development, and stratigraphy. He also assigned ages to the surfaces by correlating the soils to other chronosequences that had numerical age constraints. Boulders from four of the geomorphic surfaces were sampled for ^{36}Cl buildup dating. In this case ^{36}Cl buildup dating could not provide absolute ages to any of the surfaces with any degree of confidence because it appeared that the boulders were exposed to cosmic rays prior to deposition. Fluvial terraces that were obviously Holocene had mean ^{36}Cl ages of 37.2 ka and 61.5 ka. The ^{36}Cl age distributions appear to represent the average of more than one transport mechanism rather than absolute ages. However, ^{36}Cl age distributions did define a relative chronology of the surfaces which appears to agree with the one that Simpson (1991) initially suggested.

Table of Contents

List of Figures

List of Tables

Acknowledgements

I would like to express my appreciation to Beiling Liu for instruction and assistance in the Isotope Hydrology Laboratory and for sharing her hard work on the ^{36}Cl buildup calculations with me. I would like to thank Dr. Phillips for his guidance and for reviewing this manuscript and making helpful suggestions. I would also like to thank Dr. Hawley for lending his expertise for the geomorphological interpretations of the landforms studied in this research project. This research was funded by a grant from the United States Geological Survey.

Introduction

Geologists have struggled for years to assign numerical ages to geomorphic surfaces. Most efforts have been correlative in nature, which involve large uncertainties at best. Birkeland (1990) claims chronosequences of soils can be used to estimate surface ages with an accuracy of ± 30%. A soil chronosequence is a chronology of soil development on one or several geomorphic surfaces. Chronosequences and chronofunctions (time dependent soil properties such as $CaCO_3$ morphology, formation of weathering products, horizon hue, etc.) of soils rely on the assumption that time is the variable; vegetation, parent material, topography, and climate are constant. This assumption introduces error because it is impossible to keep all soil forming factors except time constant for all the soils of a chronosequence. Climatic change alone would lead one to conclude that soils older than ten thousand years are most likely polygenetic. Furthermore, correlating one soil chronosequence to another one that may not even be in the same drainage compounds the error. Because most alluvial environments fail to preserve adequate amounts of material suitable for ^{14}C dating, geologists are often forced to correlate geomorphic surfaces to estimate the age of a surface. In situ accumulation of cosmogenic nuclides (such as ^{36}Cl) could potentially decrease the error involved in estimating the age of a surface.

Estimating Geomorphic Surface Ages

There are three basic categories of methods for dating exposed surfaces: (1)correlative methods , (2) relative age methods, and (3) chemical or physical techniques. One particular correlative method, soil chronosequence, was discussed above. Soil chronosequences can provide estimates for surface ages, but as Birkeland (1990) points out, this method needs refinement. Improvements lie in finding better dating controls, finding independent evidence for climatic change, and defining the error in estimation of deposit ages from various kinds of soil data. Correlative and relative dating techniques involving soil development are by far the most common methods presently used. The rest of this section will summarize chemical or physical techniques available.

Dorn (1991) has successfully used rock varnish to estimate exposure ages of rocks. This involves extracting the organic layers in the varnish and dating them by the ^{14}C method (The ^{14}C method has a range of 5000 to 40,000 years). Dorn (1991) also used the (Na+Ca):Ti ratio in the varnish layers as a relative dating technique. Dorn (1991) is careful to point out that varnish can only give a minimum age for the surface. The rock surface must be exposed for some time before the varnish can form. The time lag between the actual exposure date and the date when the varnish begins to form is determined by the local environmental

conditions. Decades may pass before the varnish begins to form (Dorn, 1991).

$^{230}Th/^{234}U$ dating of pedogenic carbonate presents many difficulties in obtaining a reliable age. Illuvial additions of young or ancient carbonate or removal of carbonate during leaching episodes is a challenge to avoid. Samples must be taken from the innermost lamellae in a carbonate pebble sealed off from moisture sources. Although ^{230}Th is very immobile, ^{234}U is highly mobile and can be added to the soil with each infiltration event.

With a half life of 1.5×10^6 years, the meteoric ^{10}Be buildup in soil looks like a promising alternative dating method, but it is still in its developing stages. Pavich et al (1986) determined that ^{10}Be has a residence time of around 100 ka in clay. Except for loss through erosion, decay, and runoff, most of the ^{10}Be is retained in the top few meters of soil. However, it is impossible to estimate an age for a soil that is older than 200 ka if there is no information available on paleoclimatic variation and runoff. This restricts the use of ^{10}Be to clay accumulating soils younger than 200 ka. Furthermore, Pavich et al (1986) state that a better understanding of how ^{10}Be enters the soil and its mobility is needed to increase this method's reliability.

In situ accumulation of cosmogenic nuclides begins as soon as a rock is exposed to cosmic rays. Eventually the ratio of unstable to stable isotope (R) in the rock will reach

secular equilibrium (R_{sec}) with the production and the decay of the unstable isotope. R_{sec} may be calculated if the altitude and the chemical composition of the rock is known. Secular equilibrium $^{36}Cl/Cl$ ratios for most rocks at sea level are on the order of 10^{-11} (Bentley et al, 1986). Observed ratios in rocks are usually at least an order of magnitude lower than this which would indicate exposure age or weathering rates. Chlorine-36 ($t_{1/2}$ = 3 x 10^5 years), ^{10}Be, and ^{26}Al buildup dating have a relatively simple sampling criterion. It is only necessary to sample suitable boulders that are fully exposed to cosmic rays and have been in a geomorphically and tectonically stable environment since their exposure to cosmic rays. A detailed discussion of ^{36}Cl production mechanisms and exposure age calculations is presented in the procedures and methods section.

Geologic Setting

The region of study is the Organ Pipe Cactus National Monument in southern Arizona, approximately 120 km west of Tucson. It lies in the Ajo Volcanic Field. The Ajo Volcanic Field covers an area of 5000 km^2 and extends from the Mexican border to just north of US Interstate Highway 8 and from the Growler and Aguila Mountains in the west to the Vekol - San Simon Valleys on the east (see Figure 1). This volcanic field consists of mostly Tertiary lavas that include the entire compositional range from basalt to

rhyolite. Gray and Miller (1984), have divided these rocks into three sequences:

(1) The oldest sequence is Oligocene to early Miocene in age. It consists of red fanglomerate and coarse arkosic sandstone intercalated with andesite, rhyolite, rhyodacite, and local pyroclastic rocks.

(2) The intermediate sequence is early to mid Miocene in age. It consists of basalt, latite, silicic flows, and associated pyroclastic rocks.

(3) The youngest sequence is mid Miocene in age. It consists of basaltic andesite and andesite.

The middle sequence is the most widespread. Its oldest rocks are rhyolitic to rhyodacitic flows and pyroclastic tuffs. Jones (1974) published a K-Ar age of 15.4 million years for the rocks on Mt. Ajo, which is one of the mountains that bounds the study region. Gray and Miller (1984) provide K-Ar ages for the following mountain ranges: 18.7 ± 5 my for the southern Growler Mountains, 16.1 ± 0.7 my for the western Ajo Range, and 16.7 ± 0.8 my for the Bates Mountains.

Figure 1, A generalized map of the Ajo area (from Gray and Miller, 1984)

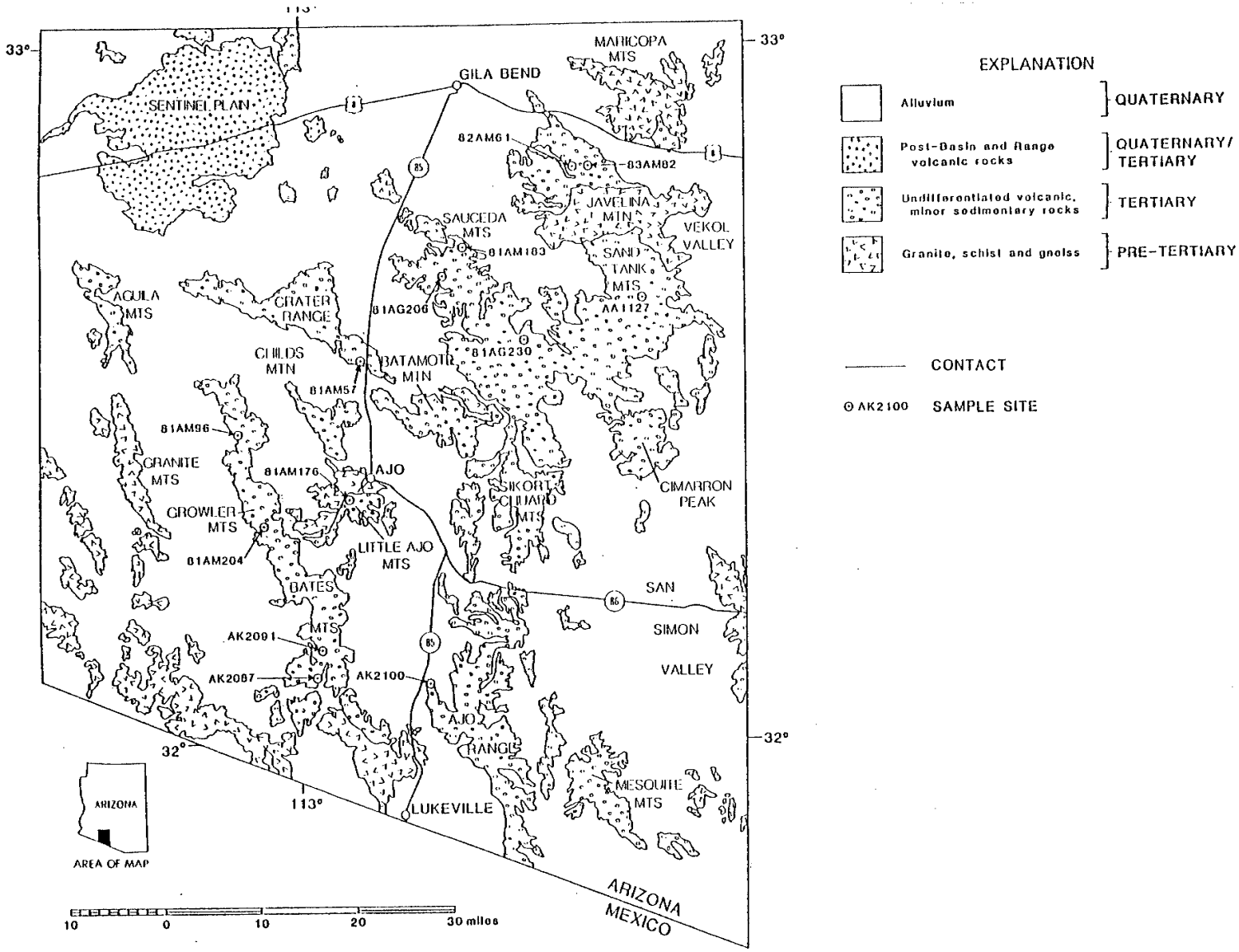

Climate

The monument is in the northeastern edge of the Sonoran Desert where the average daily temperature is 15-20^{0}C from December to February, and usually exceeds 38^{0}C from May to October. Average annual precipitation is 25 cm at the U.S. National Park Service Visitor's Center where the elevation is 510 meters. Most of the precipitation falls in summer or winter. Winter frontal storms give light but steady rainfall while summer monsoons are very localized, heavy and brief thunderstorms. Late spring is known for being especially dry.

Vegetation

Natural vegetation in the North American deserts is typically described in terms of vegetation zones (Hendricks, 1985). The study region is in the Sonoran vegetation zone, two thirds of which lies in north western Mexico. The Organ Pipe Cactus National Monument lies in the Arizona Upland Division. Representative vegetation includes saguaro cactus, organ pipe cactus, cholla cactus, ocotillo, foothill and blue paloverde, ironwood, mesquite, and creosotebush.

Previous Investigations

Simpson (1991) distinguished six morphostratigraphic units in this region in his master's thesis based on topographic relief, surface morphology, stone pavement development, and

stratigraphy. He assigned approximate ages to the surfaces by evaluating their soil development and correlating them to well known soil chronosequences found in the Soda Mountains, Harqualhala Mountains, and the Canada del Oro Valley, where numerical age constraints were available. (See Figure 2 for Simpson's map) For the purposes of this study, only four of Simpson's surfaces will be considered. A summary of Simpson's descriptions for those surfaces are provided in Table 1.

Simpson estimated that Qf1, the oldest alluvial fan surface, was mid to early Pleistocene. Qf2 (an alluvial fan) and Qt1 (an aggradational terrace) formed during the mid Holocene to the latest Pleistocene, with Qt1 forming subsequent to Qf2. Qt2 could have formed during the mid Holocene or in the most recent centuries.

Figure 2, Map of geomorphic surfaces of the study area (modified from Simpson, 1991)

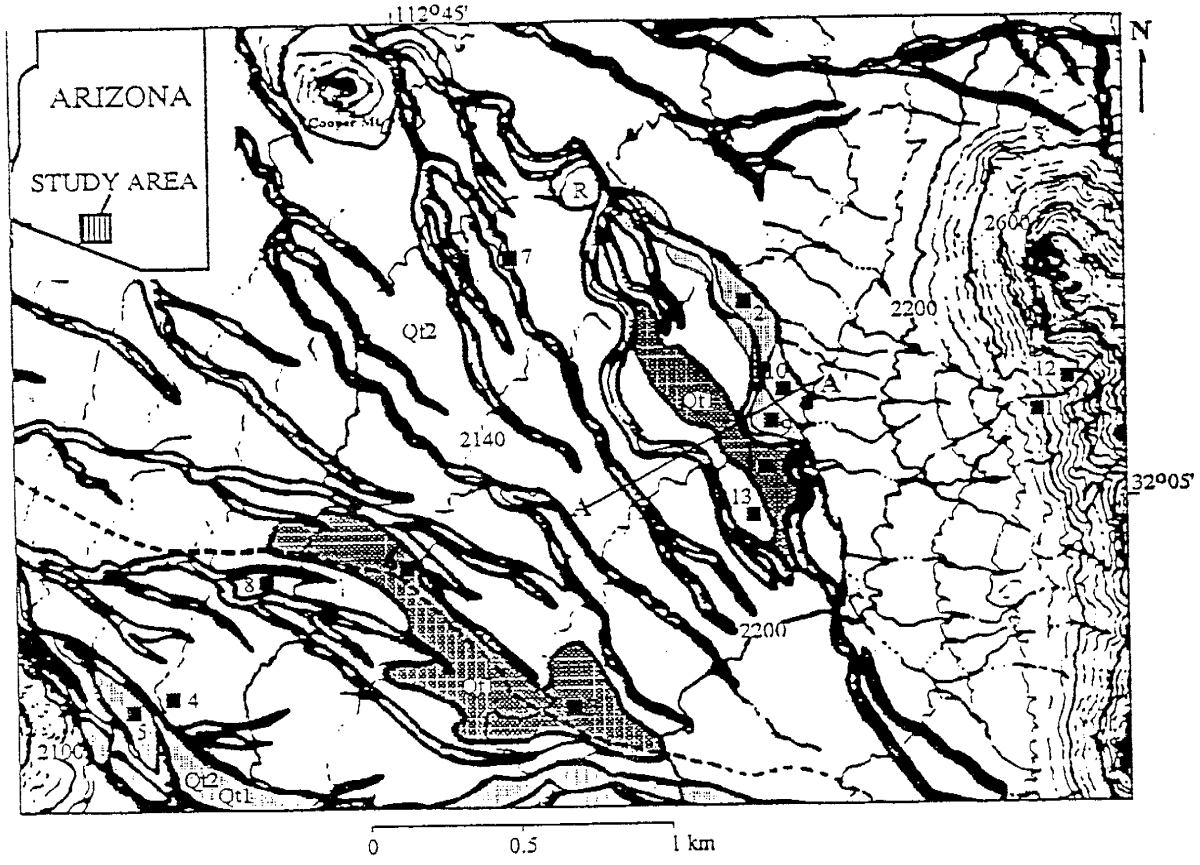

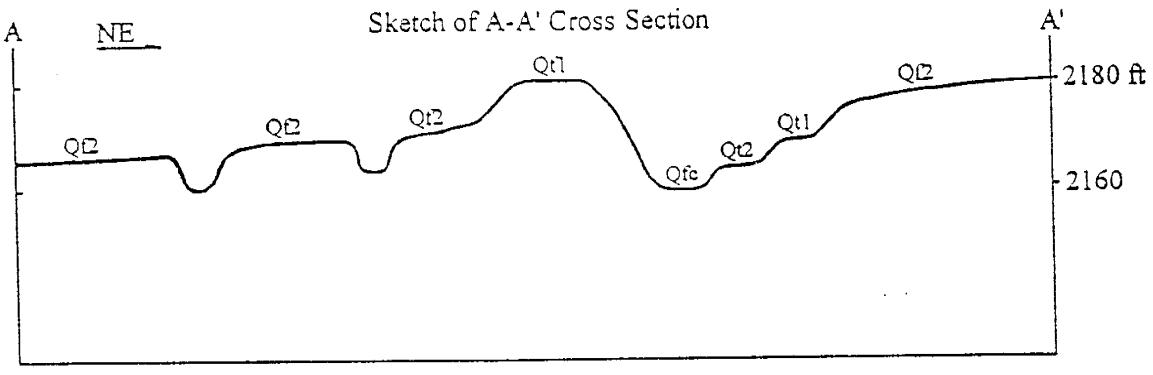

Surface	Topography	Morphology	Stone Pavement	Stratigraphy	Soil description
QF1	The highest surface on piedmont. Ballena topography	A group of deeply dissected remnants of proximal parts of alluvial fans that used to be more extensive and headed from the Ajo Mountains.	Poor	Thin gravelly silty or sandy loam soil over massive, indurated cobble/ gravel petrocalcic horizon.	A horizon > 30 cm thick. K horizon ≈ 5m thick. Composed of aeolian dust, residual sand, gravel, and petrocalcic rubble from the old soil which was eroded from underlying petrocalcic horizon (stage IV carbonate morphology).
QF2	Below QF1 but above everything else.	Fan covers 80% of piedmont. Proximal & medial regions gently sloping to flat. Distal areas are broader, flatter, & fewer drain-age channels.	A few areas have 1/3 of the surface armored. This is the best pavement exhibited in the study area.	Soils on top of stage IV petrocalcic horizon of QF1. Little petrocalcic rubble present on QF2.	30-80 cm deep. Thin A horizon. Gravelly loam and clay loam Secondary carbonate (stage I to II) Abrupt A-K boundary. K horizon has a very old petrocalcic layer.
QT1	Inset below surrounding alluvial fan deposits.	Aggradational fill terrace units along Alamo Wash.	Weakly to moderately developed.	5 m thick bouldery sediments. Gravelly sand loam soils 1-1.5 m deep. No petrocalcic horizon.	Weak to moderate development; bouldery, gravelly, sandy loams. No sign of clay transformation. Secondary carbonate as rinds on gravels and is finely decimated below 28 cm.
QT2	0.5 - 2m above channel.	Youngest terrace unit. Low and small local berm deposits. Bar and swale.	None.	Sandy silt cap .2 - .5 m thick overlies coarser grained channel deposits.	Weakly developed incipient soil. Thin B horizon has no rubification and is noncalcareous.

Table 1, A summary of four geomorphic surfaces described by Simpson, 1991

Procedures and Methods

All of the sample preparations have been performed at New Mexico Tech. Total chloride concentrations in the rock samples were measured with the ion selective electrode with a procedure developed by Aruscavage and Campbell (1983); measurements were made in the Isotope Lab of the Hydrology Program, New Mexico Tech (see the lab procedure section of this paper). The major elements were measured by X-ray fluorescence spectrometry with an analytical uncertainty better than 2% for all critical elements. Major element measurements were made by the X-ray Assay Laboratories Limited in Ontario, Canada. Inductively coupled plasma atomic emission spectrometry was used to determine B and Gd concentrations. Boron and Gd measurements were made by XRAL Activation Services Inc. in Ann Arbor, Michigan and the X-ray Assay Laboratories Limited. Chlorine-36 was analyzed by accelerator mass spectrometry at the Nuclear Structure Research Laboratory, University of Rochester.

Chlorine-36 Buildup Dating

Chlorine-36 is produced in surface rocks from spallation of K and Ca and activation of ^{35}Cl by cosmic ray derived thermal neutrons. The amount depends on the latitude, exposure time, altitude, target element abundance, and weathering rate. A summary of the theory behind Chlorine-36 buildup dating is given below.

Cosmic rays

The upper atmosphere is constantly bombarded with high energy particles from outside the solar system and the sun (photons, electrons and nuclear particles). Secondary radiation results from these particles hitting atoms in the atmosphere and producing more particles, such as pions and neutrons. Pions have a mean lifetime of only 2.6e-8 sec, so most decay before reaching the surface of the earth (Aguilar-Benitez et al., 1990). Pions decay into a muon and a neutrino. Traveling at nearly the speed of light, ($\approx$ .998c) many muons reach the earth before they decay (Gregory and Clay, 1991). Muons can have extremely high energies, but interact only weakly with atoms in the atmosphere. Neutrons make up a major part of the cosmic ray flux at high altitudes. Neutrons directly interact with nuclei and produce disintegrations; they are thus attenuated much faster in the atmosphere than muons. At sea level, the cosmic ray flux has comparable amounts of neutrons and negative muons (Rama and Honda 1961). Approximately 50% of the cosmic rays are absorbed by the top 40 cm of the lithosphere.

Production Reactions

When a nucleon (a nuclear particle) strikes a nucleus, several processes can occur. The type of process that will occur depends on the energy of the nucleon, the size of the

nucleus, the angle at which the nucleon strikes the nucleus, etc. The processes can be divided into two basic categories, absorption and scattering.

Absorption happens when the incident nucleon is absorbed by the nucleus and a new compound nucleus is formed. This new compound nucleus is often unstable and will fall to a state of lower energy and emit radiation and/or new particles.

Scattering can be elastic or inelastic. Elastic scattering conserves momentum and kinetic energy. It is often described as a "billiard ball" type collision. Inelastic scattering occurs when some of the kinetic energy of the incident nucleon is absorbed by the nucleus. This raises the nucleus to an excited state and it will emit energy in the form of γ rays and/or nuclear particles. If the incident nucleon energy is high enough, new particles (mainly pions), may be generated in a collision with an individual nucleon in the nucleus.

The probability of a particular nuclear interaction occurring is expressed in terms of an effective area of cross section of the nucleus. Cross sections are often expressed in units of 10^{-24} cm^2 (barns). There will be a cross section value for each type of interaction (such as scattering, absorption, etc.) for each nucleus, such that if an incoming particle penetrates this area, the interaction will take place. In other words, the cross section is not a

geometric area but a fictitious area that will describe the area of each nuclear interaction for each element.

Chlorine-36 is produced in rocks exposed to cosmic rays through thermal neutron activation of ^{35}Cl, spallation of ^{39}K and ^{40}Ca, and slow negative muon capture by ^{40}Ca. Chlorine-35 is not a particularly abundant element in most rocks, but it has a very large neutron absorption cross section (43.7 barns (Holden, 1990)) which enables measurable ^{36}Cl production. The major sources of thermal neutrons are from cosmic rays and from decay processes of elements in the U-Th series (Bentley et al., 1986). Potential sinks for the thermal neutrons (besides ^{35}Cl) are elements with huge neutron absorption cross sections such as gadolinium (4.88×10^4 barns) or boron (7.6×10^2 barns) (Holden, 1990). Thus, to calculate ^{36}Cl production due to thermal neutron activation of ^{35}Cl, one must account for thermal neutron availability.

Slow negative muon capture is an absorption type interaction while spallation is inelastic scattering. Negative muons fall into the K shell of the atom and have a finite probability of being captured by the nucleus before they decay (Rama and Honda, 1961). This probability depends on the atomic number of the target element (Rama and Honda, 1961). Spallation occurs when an incoming particle has sufficient energy to cause nuclear disintegrations when it makes a direct hit on the nucleus of an atom. Existing data

on cross sections for these two nuclear interactions is insufficient to permit precise calculations of ^{36}Cl production. Thus, empirical methods were developed for calculating the ^{36}Cl production rate due to spallation and slow negative muon capture (see Zreda et al. (1991) or Lal (1991)). Independently dated rocks or minerals with very high concentrations of a specific target element were analyzed for ^{36}Cl and major and minor trace elements in order to measure an effective production rate due to a particular nuclear reaction.

Top Meter of Lithosphere

Table 2 shows that thermal activation of ^{35}Cl and spallation of ^{39}K and ^{40}Ca dominate ^{36}Cl production. Note that the relative contribution of a production reaction depends on the chemical composition of a rock.

Table 2
Relative importance of major reactions producing ^{36}Cl in the top 0.5 m of water equivalent (mwe) of the lithosphere at sea level in crustal rocks (from Zreda et al. 1991)

Reaction Type	Notation	% of Total ^{36}Cl
Spallation of K and Ca	$^{39}K(n,2n2p)^{36}Cl$ $^{40}Ca(n,2n3p)^{36}Cl$	16 - 80
Thermal neutron activation of Cl	$^{35}Cl(n,\gamma)^{36}Cl$	11 - 80
Negative muon capture by Ca	$^{40}Ca(\mu^-,\alpha)^{36}Cl$	0.3 - 10
Thermal neutron activation of K	$^{39}K(n,\alpha)^{36}Cl$	0 - 2
Negative muon capture by K	$^{39}K(\mu^-,p2n)^{36}Cl$	0 - 0.4

Below One Meter

Negative muon capture becomes progressively more important with depth. The heavier particles (such as neutrons) interact more strongly with the atoms in the rock or soil than the muons; heavy particles are attenuated quicker than the muons. Thus the muon portion of the cosmic ray flux increases with depth. Below 1.0 kg cm^{-2}, muon capture exceeds thermal neutron capture. At approximately 5 kg cm^{-2}, thermal neutron capture practically disappears and muon capture is the dominant ^{36}Cl production reaction. (Lal and Peters, 1967)

Calculations

Assuming that erosion is negligible, the amount of cosmogenic ^{36}Cl accumulated in a rock exposed to cosmic rays after t years is calculated as follows (Zreda et al., 1991):

$$R - R_0 = \frac{E_n L_n D_n (\psi_K C_K + \psi_{Ca} C_{Ca} + \Psi_n) + E_{\mu^-} L_{\mu^-} \Psi_{\mu^-}}{\lambda N} \times (1 - e^{-\lambda t}) \quad \textbf{(1)}$$

Where:

R = atomic ratio of ^{36}Cl to stable Cl

R_0 = background $^{36}Cl/Cl$ resulting from U and Th derived neutrons. R_0 is usually small, around 5×10^{-15} to 5×10^{-14} $^{36}Cl/Cl$ (Bentley et al., 1986). R_0 is only important for rocks with very short exposure times.

ψ_K, ψ_{Ca} = production rates due to spallation of ^{39}K and ^{40}Ca, in atoms (kg of rock)$^{-1}$ yr^{-1} per unit concentration (w/w) of K or Ca, at sea level and geomagnetic latitude ≥ 60°. A new estimation of ^{36}Cl production rates due to spallation of ^{39}K (ψ_K = 1700 atoms (kg of rock)$^{-1}$ yr^{-1} per % weight of K_2O in rock) and ^{40}Ca (ψCa = 515 atoms (kg of rock)$^{-1}$ yr^{-1} per % weight of CaO in rock) was made by Zreda (1993, paper in progress) and was used in the calculations for this paper.

C_K, C_{Ca} = concentration of K or Ca (w/w)

Ψn = production rate due to thermal neutron activation of 35Cl in atoms (kg of rock)-1 yr^{-1} , at sea level and geomagnetic latitude ≥ 60°. Where:

$$\Psi_n = \phi_n \frac{\sigma_{35} N_{35}}{\Sigma \sigma_i N_i} \qquad (2)$$

σ = the thermal neutron absorption cross section

N = the atomic concentration.

ϕ = Time-integrated thermal neutron capture rate (n* kg rock^{-1} * yr^{-1}). Literature values range from 2 x 10^5 to 4 x 10^5. Zreda et al, (1991) estimated ϕ to be 3.07 x 10^5. The revised integrated thermal neutron capture rate used in this study is 3.13 x 10^5.

Ψ_{μ^-} = production rate due to slow negative muon capture by ^{40}Ca, in atoms (kg of rock)$^{-1}$ yr^{-1} , at sea level and geomagnetic latitude ≥ 60°

E, L, and D = scaling factors for the dependence of the cosmic ray neutron (n) and muon (μ-) fluxes on elevation above sea level (E), geomagnetic latitude (L), and depth below surface (D)

t = time of exposure in years

N = stable Cl concentration in atoms per kg of rock

λ = decay constant for ^{36}Cl (2.30×10^{-6} yr^{-1})

Zreda et al (1991) state:

"E_n, the scaling factor for neutron above sea level and L_n, the scaling factor for neutrons' geomagnetic latitude can be calculated based on the work of Lal (1967), Yokoyama (1977), and several others. D_n, the scaling factor for neutrons below the surface, is expressed as exp(-depth/Λ_n). Λ_n is the mean free path of the neutrons and ranges from 150 - 160 g/cm^2."

Lab Procedures

Chloride Measurement in Silicic Rocks

This procedure is basically the same one described by Aruscavage and Campbell (1983). A small amount of rock powder (approximately 0.2 g) is dissolved in hydrofluoric acid in a gas diffusion cell. The gas diffusion cells are 2.5 inch diameter containers (1.5 inches tall) machined from a solid cylinder of teflon. The cells have tightly-fitting teflon lids. Each cell has a circular inner chamber to

store a reducing solution; the sample and acid are stored in the outer ring chamber. Once a cell is loaded, it is shaken for 24 hours; during this time the sample is decomposed, chlorine is distilled from the rock matrix, and the chloride from the gas is collected in the reducing solution. The reducing solution is a basic sulphite solution and is a suitable medium for chloride selective electrode measurements. A step by step procedure used in the lab is given below.

Sample Preparation

- Clean the rock surfaces using a wire brush.
- Put the sample in 10% HNO_3 for at least 2 hours.
- Rinse the sample in deionized water and dry it.
- Grind the sample using the jaw grinder. Put the powdered sample in a plastic bag.
- Grind the sample using the TEMA mill.
- Take 20 grams of powdered sample for major elements analysis and place it in a brown plastic bottle.
- Mix the sample with deionized water in a 600 ml glass beaker in a proportion of 1:2 or so.
- Stir the mixture for 10 minutes using a blender.
- Leave the sample in this water for 24 hours.
- Decant the water and rinse the sample 3 times using deionized water.
- Dry sample at 100°C.
- Take 3 grams of the sample and for total Cl measurements and place in a small glass vial.

- Put the rest of the sample in a new plastic bag.

The purpose of leaching the ground up sample is to remove any meteoric chloride from the pores or grain boundaries.

Total Chloride Determination

- Clean the teflon diffusion cells using: (1) H_2SO_4 + $K_2Cr_2O_7$, (2) deionized water, (3) hot HNO_3 + H_2O_2, (4) deionized water.
- Prepare two standards: 100 ppm and 500 ppm in clean teflon centrifuge tubes. For samples with low Cl content prepare separate standards.
- Write down cell numbers and sample names in the appropriate columns in the form designed for this experiment.
- Prepare blank by weighing 2.8 g of reducing solution into the inner chamber of a teflon diffusion cell.
- Weigh 0.2 g of a standard (or sample) into the outer chamber of the teflon diffusion cell. Record the actual sample mass in the form designed for this experiment in the column "Initial Mass"
- Weigh 2.8 g of the reducing solution into the inner chamber of the teflon diffusion cell.
- Prepare the oxidizing solution in a plastic beaker. The solution contains: 0.4 g $KMnO_4$ + 5.6 g H_2O + 2.4 ml of 50% H_2SO_4 + 32 ml of HF.
- Place the diffusion cells under the hood and add 3 ml of oxidizing solution to the outer chambers of diffusion cells using a plastic pipette.
- Place all the diffusion cells on the orbital shaker and set the speed at 100 and shake the cells for 20 to 24 hours.
- Change filling solution in the ion selective electrode.
- Open the blank, pipette off the solution from the outer chamber using a small plastic pipette.
- Weigh the cell and calculate the mass of the reducing solution left in the cell. Record the reducing solution mass in the column "Final mass".

- Put the electrode in the blank solution for 30 minutes. the bottom of the electrode should be fully immersed in the solution but should not touch the bottom of the diffusion cell. Record potential at the beginning and the end of this period in the column "mV".
- Open the diffusion cells (one at a time) and remove the outer chamber solution using a plastic pipette.
- Weigh the cell, calculate the mass of the reducing solution and record this mass in the column "final mass".
- Rinse the electrode in deionized water and remove any droplets of water present.
- Put the electrode in the inner chamber of the diffusion cell so that it is fully immersed but does not touch the bottom of the diffusion cell.
- Observe potential readout for 4 minutes and record it when it is stable in the column "mV". Stability is achieved after approximately 1 minute for samples containing more than 100 pm of Cl, and after 3 to 5 minutes for samples with lower Cl concentrations.
- Rinse the diffusion cell using deionized water and put the cap on.

Chlorine-36 Measurement

Chlorine-36 Extraction

Zreda, et al, (1991) include a description of a wet chemical technique for extraction of Cl from silicate rock in their paper. However Zreda has simplified it since then. The principles are still the same. A step by step procedure followed in the lab is given below.

- Clean 1 liter teflon bottles using "Fantastik" and a soft sponge. Rinse first in tap water then three times in deionized water. Clean again using HNO_3 + H_2O_2 and then rinse using deionized water.

- Weigh appropriate amount of sample. This amount depends on the Cl concentration in the sample:

[Cl] (in ppm) in rock sample	Sample mass (g)
< 25	100
from 25 to 100	$120 - 0.8 \times C_{Cl}$
> 100	40

- Put the sample in a teflon bottle.
- Add HNO_3 in proportion 1 part of HNO_3 to 1 part sample.
- Add HF in proportion 2.5 parts HF to 1 part sample. Do not add all of the HF at once. The reaction between the rock powder and the HF is potentially violent. Add only 20 mls at first.
- Immediately close the bottle (not very tight) and leave it under the hood. Do not place it on a hot plate. Do not shake it at this time. The bottle will get hot and then cool down. Keep adding HF in small increments until all the HF has been added.
- When the bottle is cold, seal tightly and put it in a hot bath at about 80 °C. Keep it on until the sample is completely dissolved, which usually takes 24 or more hours. The sample should look like a white gell when it is completely dissolved.
- After complete dissolution, move the white gell and the liquid in the teflon bottle to a 250 ml teflon centrifuge tube. If the Cl concentration in the sample is quite high, just decant the solution into the centrifuge tube. If the sample has a very low Cl concentration, everything in the bottle must be centrifuged.
- Centrifuge at 7500 rpm for 10 minutes.
- Decant the supernatant to another 250 ml teflon bottle and add 10 ml of 0.1 M solution of $AgNO_3$.
- Place the bottle in the hot bath for about 2 hours to flocculate AgCl.
- Centrifuge the bottle immediately for 10 minutes at 7500 rpm.

- Carefully decant the solution and keep the precipitate which is AgCl.
- Rinse the AgCl in deionized water and transfer to a 50 ml teflon centrifuge tube.
- Dissolve AgCl in concentrated NH_4OH and add 1.5 ml of $Ba(NO_3)_2$ to precipitate $BaSO_4$. Leave the solution for at least 8 hours (but preferably longer). This is done to remove ^{36}S, an interfering isobar in the AMS measurement.
- Add a sufficient amount of HNO_3 to precipitate AgCl. Let it stand for 2 hours. Remove the acidic solution and rinse the AgCl three times in deionized water. Make sure the pH of the final rinse is about 7.
- Transfer the AgCl onto a clean watch glass. Remove excess water by using a small glass pipette. Cover the glass with aluminum foil.
- Place the sample in the oven for 24 hours. Set the temperature to about 60 °C.

Small samples (less than 2 mg of AgCl) were mixed with a low sulfur AgBr binder in proportion not exceeding three parts of AgBr to one part of AgCl. Dry samples are loaded into custom-made low sulfur tantalum holders.

AMS Measurements

The samples were analyzed for ^{36}Cl by accelerator mass spectrometry on the tandem Van de Graaff accelerator at the University of Rochester (Elmore et al., 1979). The analytical error was usually better than 15%.

Results

A summary of the ^{36}Cl data is presented in Table 3. S5 and S3 are surface fragment samples. Deb means the sample was taken from a debris flow channel. The bedrock sample is listed as Bed. The reference # is the location of the sampling site marked on the map (Figure 2) provided in this paper. Complete chemical analyses of the boulder samples are listed in the appendix.

Figure 2 shows Simpson's map of geomorphic surfaces copied onto a USGS topographic map with the sample locations marked on it. Locations #1, #6, and #3 are the sampling sites for the oldest alluvial fan surface, Qf1. Locations #8, #10, #13, and #4 are sampling sites for the most extensive surface, Qf2. Locations #2, #5, and #7 are the sampling sites for the youngest terrace unit, Qt2. Locations #9 and #2 are sampling sites for the older terrace unit, Qt1. Location #11 is the sampling site for the debris flow levee and channel. Location #12 is the site of the bedrock sample on the piedmont slope near the debris flow levee.

Chronology

Table 3 indicates that samples from Qt2 are around 35 ka except for two samples, one of 12.6 ka and another at 60 ka. Qt1 ranges from 32.8 ka to 95.8 ka with an average of 61.5 ka. The ^{36}Cl ages are apparently much older than the

Sample #	Unit	Ref. #	Altitude m	EL_n	$\Sigma\sigma_i N_i$ cm^2/kg	Cl ppm	K_2O %	Ca_2O %	$^{36}Cl/Cl$ $x10^{-15}$	Age $x10^3yr$
OP 90-7	QT2	2	640	1.41	7.43	44.6	4.12	3.99	233 ± 20	12.6 ±1.1
OP 90-8	QT2	2	640	1.41	5.34	33.4	4.71	1.37	599 ± 41	25.3 ±1.8
OP 90-9	QT2	2	640	1.41	7.96	58.8	4.18	4.29	488 ± 41	33.9 +3.0/-2.9
OP 90-10	QT2	2	640	1.41	4.82	50.2	4.72	1.08	683 ± 40	41.6 ±2.6
OP 91-3	QT2	5	630	1.40	6.15	121	3.66	2.7	266 ± 18	36.9 ±2.6
OP 91-4	QT2	5	630	1.40	8.81	72.8	4.51	3.09	320 ± 14	27.2 ±1.2
OP 91-5	QT2	5	630	1.40	5.55	341	5.00	1.05	268 ± 23	60.2 +5.6/-5.5
S5 #1	QT2	7	630	1.40	5.50	36.8	4.56	1.74	855 ± 59	40.7 +3.0/-2.9
OP 392-2	QT1	9	650	1.42	5.85	84.1	3.29	3.56	517 ± 21	55.8 ±2.4
OP 392-3	QT1	9	650	1.42	5.88	79.1	4.18	2.41	972 ± 69	95.8 +7.7/-7.5
OP 1092-5	QT1	2	650	1.42	5.11	49.8	3.37	3.21	474 ± 31	32.2 ±2.2
OP 91-1	QF2	4	640	1.41	5.36	57.4	6.23	1.62	2050 ±167	127 ±12
OP 91-2	QF2	4	640	1.41	5.56	86.4	3.35	3.72	1051 ±35	125 ± 5
OP 392-4	QF2	10	660	1.43	9.15	63.9	4.21	3.80	1010 ±40	81.3 +3.6/-3.5
OP 1092-3	QF2	13	660	1.43	4.62	36.8	4.51	0.79	971 ± 45	47.3 ± 2.3
S3 #1	QF2	8	650	1.42	5.28	42.2	4.49	1.05	605 ± 71	33.1 +4.1/-4.0
OP 90-1	QF1	1	650	1.42	5.05	57.4	2.03	2.21	1009 ±78	121 ± 11
OP 90-2	QF1	1	650	1.42	6.09	1226	4.28	1.56	863 ± 68	489 +78/-66
OP 90-3	QF1	1	650	1.42	4.95	55.5	5.31	1.23	1978 ±130	131 ± 10
OP 90-5	QF1	1	660	1.43	6.35	110	3.60	3.40	349 ± 22	44.0 ±2.9
OP 90-11	QF1	3	650	1.42	5.30	35.7	5.27	2.19	5191 ±379	262 +27/-25
OP 90-12	QF1	3	660	1.43	6.35	110	3.60	3.40	349 ± 22	44.0 ± 2.9
OP 90-13	QF1	3	670	1.44	5.97	55.1	3.60	2.76	2399 ±150	216 +18/-17
OP 91-6	QF1	6	650	1.42	6.58	71.6	3.48	3.29	1223 ±139	127 +17/-16
OP 91-7	QF1	6	650	1.42	5.08	36.5	4.55	3.68	2131 ±186	95.1 ± 9
OP 392-5	Qfc	11	730	1.51	5.20	36.3	4.32	1.43	840 ± 80	41.7 ± 4.2
OP 392-12	Deb	11	730	1.51	7.25	38.6	3.85	4.75	517 ± 75	25.1 +3.8/-3.7
OP 392-13	Deb	11	730	1.51	8.16	46.3	3.72	4.29	442 ± 22	26.9 ± 1.4
OP 1092-1	Deb	11	730	1.51	7.08	54.7	3.82	3.93	182 ± 8	12.4 ± 0.6
OP 1092-2	Deb	11	730	1.51	6.85	65.6	3.59	4.19	103 ± 10	8.3 ± 0.8
OP 392-10	Bed	12	780	1.57	7.66	49.4	3.33	4.81	550 ± 62	37.3 ± 4.4

Table 3, ^{36}Cl Ages and Relevant Parameters

Holocene, the age assigned to Qt2 and Qt1 based on their geomorphic features and soil development by Simpson (1991).

Qf1 has an age spectrum from 44 to 489 thousand years with an average age of 95.1 thousand years. Qf2 has an age spectrum of 33 to 127 thousand years with an average age of 82.8 thousand years.

Are the ages of the four surfaces significantly different? The standard error of the difference between two means can be obtained from the following:

$$\sigma_D = \sqrt{\frac{\sigma_1^2}{N_1} + \frac{\sigma_2^2}{N_2}}$$

where

σ_1 = standard deviation of the first sample

σ_2 = standard deviation of the second sample

N_1 = number of items in the first sample

N_2 = number of items in the second sample

If the difference between the means of the two samples is greater than $3\sigma_D$, then it is extremely unlikely that the difference between the means arose out of chance i.e., the two means are significantly different. Table 4 lists the σ_D values for the surfaces ages below.

Table 4, σ_D for surface ages and relevant parameters.

Surfaces	Mean Age (ka)	Standard Dev. (ka)	Δ_{mean}	σ_D	$3\sigma_D$	Comments
Qf2 Qt2	82.8 38.1	38.6 11.6	44.7	17.9	53.7	Surface fragments and youngest qt2 age included
Qf2 Qt2	95.3 37.6	33 12.6	57.7	17.4	52.3	Surface fragments and youngest qt2 age excluded
Qf2 Qf1	95.3 193	33 128	97.7	45.7	137	
Qt1 Qt2	61.5 37.6	26.0 12.6	23.9	16.0	48.0	
Qf1 Qt2	193 37.6	128 12.6	155	43.0	129	

Table 4 shows that the difference between the mean age of Qt2 and Qf2 is not significant. However, if the age the surface fragment samples and the youngest sample on Qt2 were dropped, the mean ages were significantly different. The justification for dropping the youngest age on Qt2 was that it seemed like that boulder had been tipped over sometime after that surface was formed, thus giving an anomalous young age. This suspicion was supported by the fact that the large boulder sampled in the middle of the debris flow channel gave a similarly young age; very likely it was tipped over at some point. The surface fragment samples however, are the most likely to have been disturbed some time during surface development. Based on these justifications, the mean ages of Qt2 (37.6 ka) and Qf2 (95.3 ka) are significantly different.

The standard error of difference between the mean ages of Qf2 and Qf1 indicates they are not significantly different. This is not surprising because it is still uncertain whether

Qf2 is entirely an alluvial fan surface. This will be discussed in more detail in the next section.

There is no significant difference between the mean ages of Qt1 and Qt2.

Note that the maximum and average ages suggest a chronology like the one given by Simpson (1991):

Table 5, Summary of ^{36}Cl Ages

Surface	Maximum Age (ka)	Average Age (ka)	Minimum Age (ka)
Qt2	60.2	37.6	25.3
Qt1	95.8	61.5	32.2
Qf2	127	95.3	47.3
Qf1	489	193	44.0

*Note- the youngest age on Qt2 and the surface fragment samples were not included here.

Surface Fragment Samples

The purpose of sampling boulder fragments on the surface of Qt2 and Qf2 was to obtain information regarding the travel time of material from the mountains to the drainage basin. The age of the surface fragment samples from Qt2 and Qf2 is 40.7 and 33.1 ka respectively. These surface fragment samples have ages similar to the ages of a sample from a rounded boulder imbedded in the bottom of the channel (41.7 ka) and a sample of bedrock on the mountain front (37.3 ka).

Debris Flow Samples

Two boulders from a debris flow levee yielded an average

age of 26.1 thousand years while a large boulder (≈ 2 m thick) in the debris flow levee gave an age of 12.9 thousand years on its top surface and 8.7 ka on its bottom surface. One sample of a boulder exposed in the floor of the debris flow channel yielded an age of 41.7 ka. A sample of exposed bedrock on the piedmont slope near the debris flow levee gave an age of 37.3 ka.

The Qt2 Age Question

A cobble profile was sampled on Qt2 to determine if the ages obtained on that surface were a result of exposure histories prior to surface development. If the cobbles had no pre exposure history, their ^{36}Cl profile should be similar to the cosmogenic ^{36}Cl buildup profile with depth. As it turns out, the sequential ages of these cobbles are random and not dependent on depth (see Table 6). This indicates that the material making up this surface had a pre exposure history. The average age of the cobbles was 32.8 ka and their ages ranged from 20.4 ka to 63 ka.

Table 6, Cobble profile on Qt2; ages and some relevant parameters

Sample #	Depth (cm)	Age (ky)	Altitude (m)	EL_n	ρ g/cm^3
BD 1-1	5.8	43.2	640	1.41	2
BD 6	49.5	2.4	640	1.41	2.2
BD 7-3	86	63.0	640	1.41	2.2
BD 8	114	43.5	640	1.41	2.2

Samples were also systematically collected along the piedmont slope to see if the Qt2 ages represent an average transport process along the piedmont slope. Location #2 is one of the sampling sites for the Qt2 surface. The average age at this location is 28.4 ka and the ages range from 12.6 ka to 41.6 ka. Location #11 is the sampling site for the debris flow levee and channel. The range of ages and the average age is mentioned in the debris flow section above. Location #12 is the site of the bedrock sample mentioned earlier. The average age of locations #11 and #12 is 28.8 ka and the range is from 12.9 - 41.7 ka; this age distribution is very similar to the average age and range of ages for location #2.

Assumptions and Caveats

The ^{36}Cl ages are calculated based on the assumption that boulders suddenly exposed to cosmic rays have remained in a constant position without erosion. This assumption may not always be valid even though boulders were carefully chosen to meet the sampling criteria. Because the thermal neutron flux reaches a maximum at approximately 20 cm beneath the surface (Yamashita et al., 1966; O'Brien et al., 1978; Fabryka-Martin, et al., 1991), the boulders that experienced degradation generally give older apparent ages if ^{36}Cl production due to the thermal neutron activation of ^{35}Cl is significant. The boulders that experienced a previous

exposure history also give older apparent ages. On the other hand, the boulders disturbed during the surface development will more likely give younger apparent ages. If a boulder is shifted or toppled over, the cosmogenic ^{36}Cl buildup 'clock' is reset; an unexposed surface is suddenly subjected to cosmic rays after the boulder was initially deposited. Therefore, it is not surprising that the ^{36}Cl ages from a single surface are not uniform and that the more the thermal neutron activation of ^{35}Cl contributes to ^{36}Cl production, the older is the apparent age.

Discussion

Chronology

Pre-Exposure History

The boulders from the youngest surfaces definitely had a pre exposure history. Simpson (1991) assigned reasonable ages to the surfaces based on soil development, yet the ^{36}Cl ages differ considerably from his estimates. He assigned Holocene to the most recent centuries to Qt2 while the mean ^{36}Cl age is 37.2 ka. Qf2 and Qt1 were assigned and Holocene to latest Pleistocene by Simpson (1991), yet the mean ^{36}Cl ages were 95.2 ka and 61.5 ka respectively. The only ^{36}Cl age that might agree with an age assignment by Simpson (1991) is the mean age of Qf1, 193 ka (Simpson (1991) assigned Qf1 an age of mid to early Pleistocene). However, the possibility that the boulders on Qf1 had a pre-exposure history can not be ruled out. Although the surface chronology indicated by the mean and maximum ^{36}Cl ages is similar to the chronology suggested by Simpson (1991), it is impossible to assign absolute ages because of the uncertainty regarding the pre-exposure history of the boulders. Another dating technique such as rock varnish dating, is needed to constrain pre-exposure history estimation.

Qf2 vs. Qf1

Chlorine-36 buildup data show no significant differences between the mean age of Qf1 and Qf2. This could be the result of confusion over which surface is actually Qf2. Qf2 is the most extensive surface in the study region (see Figure 2). According to Simpson (1991), Qf1 was eroded down to its petrocalcic horizon and then Qf2 was deposited on top. Simpson (1991) claims Qf2 has only weakly developed soil on top of the old Qf1 petrocalcic horizon. Based on additional field observations, Dr. J. W. Hawley (communication, 1992) suggested that the underlying petrocalcic horizon is genetically related to the 'Qf2 soil'. For example, a mining exploration pit located on a surface marked as Qf2 by Simpson (1991) revealed a buried soil horizon that was in an advanced state of development overlying the petrocalcic horizon. It was a 50 cm thick argillic horizon, 2.5 YR 4/4 to 4/5 clay loam and highly structured (communication from Hawley). It is possible that areas mapped as Qf2 are actually the very top layer of Qf1 churned up. Therefore, some of the boulder samples from Qf2 may really be Qf1 samples.

Geological Processes

Since it is appears that it is not feasible to assign an absolute date to each surface based on the ^{36}Cl information obtained so far, perhaps this information should be

interpreted in terms of the geological processes at work.

Surface Fragments

There are several possibilities that could explain what the age distribution of the surface fragments. They could be an average of broken up boulders; in this case the fragments would represent a mixture of the unexposed core and the old exposed surface of boulders. They could be representative of the material that was originally deposited with the boulders and assumed to have remained in the same position since the geomorphic surface was formed. It is possible that the their ages could be a result of deposition subsequent to the boulder deposition. Their ages could be a result of the uppermost layer being churned up while the boulders stayed in place. Perhaps what is seen now is the result of erosion, not deposition.

It doesn't seem reasonable that the gravelly material was entirely a result of large boulders breaking down after deposition, while conveniently leaving several of the boulders unscathed to meet ^{36}Cl sampling criterion. It is likely that the surface fragments were disturbed since deposition, either by plants and animals, wind, or some localized erosion. However, assuming that the fragments were left undisturbed, the next question is whether the surface is depositional or if it was eroded.

The apparent age of the surface fragments on Qt2 is 40.7

+3.0/-2.9 ka and the apparent age on Qf2 is 33.1 +4.1/-4.0 ka. The two ages are similar within their limits of uncertainty. It is suspected that Qf2 may actually be the surface of Qf1, so there should be a significant difference in age between Qf2 and Qt2 surfaces. Why do the surface fragments give similar ages? Most likely the source for the gravelly material on Qt2 was the surrounding geomorphic units. The surface fragments on the piedmont accumulate ^{36}Cl for a period of time, then they are transported away and a new layer accumulates on the eroded surface. Because the other surfaces are topographically higher than Qt2, one would expect that Qt2 has the best chance of containing materials from the higher, older surfaces. Furthermore, the locus of deposition is shifted down fan because of channel incision. The higher, older surfaces are probably experiencing erosion. The range of ages for Qf2, 47.3 to 127 ka, is higher than 33.1 ka, its surface fragment age. This might suggest a residence time, the period of time between depositional and erosional events. However, because the rocks probably experienced previous exposure to cosmic rays, (as seen in the cobble profile on Qt2) estimation of a residence time would be very difficult.

It is important to note that the bedrock sample has an apparent age 37.3 ± 4.4 ka and the sample of a rounded boulder imbedded in the bottom of the debris flow channel has an apparent age of 41.7 ± 4.2 ka. These are similar to

the surface fragment ages. This may suggest a short residence time for material from the mountains down through the drainage basin.

Debris Flow

Is it possible to find the age of a debris flow? The ages of the rocks from the debris flow levee itself are similar - 25.1 ka and 27.1 ka. The two-meter-thick boulder in the channel was probably flipped over. If the age of the top surface is added to the age of the bottom surface, the total age is 21.6 ka. Even though their ages are similar, it is likely that the rocks from the debris levee were exposed to the atmosphere prior to the debris flow. According to Dr. J. Hawley, bouldery material in this situation has a short residence time so the debris flow is probably Holocene. Assuming that the bottom surface of this boulder was exposed to the atmosphere before the debris flow and then flipped over, the age calculated for the top surface (12.9 ka) could represent the approximate age of the debris flow. This could be why the sum of the ages of the two surfaces is similar to the ages obtained from the debris flow levee.

Bull (1984) points out that debris flows were fairly common in the American southwest at least four to six thousand years ago, based on desert varnish and pitting of the boulders. It would be interesting to obtain ages based

on varnish coatings from these boulders and compare their ^{36}Cl ages to their varnish ages. Climatic transition between the late Pleistocene to Holocene may have produced conditions favorable to debris flows. Either precipitation decreased or the temperature increased. Both cases would have decreased the amount of vegetation thus making it easier for debris flows to occur. Perhaps the 12.9 ka age from the top surface of the channel boulder is indicative of the age of the debris flow.

Qt2

The results for the systematic sampling of the piedmont slope show that the age distribution of Qt2 was nearly the same as the age distribution of the slope. Furthermore, the cobble profile revealed that Qt2 material had a prior exposure history. What can be concluded from Qt2's age distribution?

The ages of Qt2 probably represent an average of more than one transport process. One mechanism is obviously a debris flow. Another has to be a water laid deposit filling in channels that were incised in the fan. Note that the age of the debris levee (25.1 - 26.9 ka), the bedrock (37.3 ka), and the bottom of the debris flow channel (41.7 ka) fall within the range of Qt2 (25.3 ka - 60.2 ka). It appears that any erosional process occurring on the mountain front is represented in the Qt2 deposit.

Conclusions

Chlorine-36 buildup dating is a good method for defining the chronology of a suite of geomorphic surfaces (this has turned out to be a relative age method), but it needs additional independent information for it to be useful in estimating the actual age of the surface. Material on any given surface was exposed to cosmic rays prior to deposition. This issue will not be resolved until another method that measures exposure age such as varnish dating or ^{10}Be and ^{26}Al buildup is used as well. Therefore, in this case, the ^{36}Cl buildup method would appear to give the maximum possible age of a surface.

The chronology suggested in this paper is similar to the one suggested by Simpson (1991); Qt2 is the youngest terrace unit, Qt1 is the next oldest terrace unit, Qf2 is the next oldest surface, and Qf1 is the oldest surface. There is reason to believe that Qf1 and Qf2 may be the same surface based on field observations as well as the overlapping age distributions obtained from the ^{36}Cl buildup measurements.

The age distributions on Qt2 and Qt1 appear to represent more than one process; at least a debris flow and a water laid deposit filling in an incised channel.

Recommendations for Future Research

Erosion causes older or younger apparent ages of cosmogenic radionuclides for boulder samples depending on the erosion rate and the proportion of the production rate due to thermal neutron activation. Two or multiple radionuclides with different half-lives can provide a constraint for both the erosion rate and the actual age (Lal, 1991; Nishiizumi et al., 1991). An analysis of ^{36}Cl with another pure spallogenic radionuclide has a good practical application for studying erosion and dating (Liu, et al., in preparation). Boulder samples from Qf1 and Qf2 should be collected to measure ^{10}Be (or ^{26}Al) and ^{36}Cl in order to constrain erosion rate and exposure history estimates.

Age estimates from rock varnish would be extremely useful on the debris flow levee and other surfaces with sufficient varnish. Again, this would help delineate pre exposure history.

References

Aguilar-Benitez, M., R. M. Barnett, C. Caso, G. Conforto, J. J. Eastman, R. A. Eichler, D. E. Groom, K. Hagiwara, K. G. Hayes, J. J. Hernandez, K. Hikasa, G. Hohler, S. Kawabata, G. R. Lynch, L. Montanet, R. J. Morison, K. A. Olive, F. C. Porter, A. Rittenberg, M. Roos, R. H. Schindler, K. R. Schubert, R. E. Shrock, J. Stone, M. Suzuki, N. A. Tornqvist, T. G. Trippe, C. G. Wohl, G. P. Yost, B. Armstrong, K. Gieselmann, and G. S. Wagman. 1990. Summary Tables of Particle Properties. *CRC Handbook of Chemistry and Physics*, 72nd Edition. D. R. Lide, ed. CRC Press, USA. pp 11-4

Aruscavage, P. J. and E. Y. Campbell. 1983. An Ion-Selective Electrode Method For Determination Of Chlorine in Geological Materials. *Talanta.* 30: 745-749

Bentley, H. W. , F. M. Phillips and S. N. Davis. 1986. Chlorine-36 in the Terrestrial Environment. *Handbook of Environmental Isotope Geochemistry*, Vol 2, *The Terrestrial Environment.* B. P. Fritz and J.-Ch. Fontes, eds. pp 422-480, Elsevier, New York, N. Y.

Birkeland, P. W. 1990. Soil Geomorphic Research - a Selective Overview. *Geomorphology III.* Elsevier Science Publishers BV, Amsterdam

Bull, W. B. 1984. Alluvial Fans and Pediments of Southern Arizona. Landscapes of Arizona, the Geological Story. University Press of America

Dorn, R. I. 1991. Rock Varnish. *American Scientist.* 79:542-553

Elmore, D., M. R. Clover, J. R. Marsden, H. E. Gove, H. Naylor, K. J. Purser, L. R. Kilus, R. P. Beukins, and A. E. Litherland. 1979. Analysis of ^{36}Cl in Environmental Water Samples Using an Electrostatic Accelerator. *Nature.* 277: 22-25

Fabryka-Martin, J. F., M. M. Fowler, and R. Biddle. 1991. Study of Neutron Fluxes Underground. *Los Alamos National Laboratory, Isotope and Nuclear Chemistry Division, Quarterly Report*, October 1 - December 31, 1990. pp 82-85

Gray, F., and R. J. Miller. 1984. New K - Ar Ages of Volcanic Rocks near Ajo, Pima, and Maricopa Counties. *Isochron/West* 41:3-6

Gregory, A. and R. W. Clay. 1992. Cosmic Radiation. *CRC Handbook of Chemistry and Physics*, 72nd Edition. D. R. Lide, ed. CRC Press, USA. pp 11-133 to 11-137

Hendricks, D. M. 1985. *Arizona Soils*. College of Agriculture, University of Arizona, Tucson, pp 33-53

Holden, N. E. 1991. Table of the Isotopes. *CRC Handbook of Chemistry and Physics*, 72nd Edition. D. R. Lide, ed. CRC Press, USA. pp 11-28 to 11-132

Jones, W. C. 1974. General Geology of the Northern Portion of the Ajo Range, Pima County, Arizona. *MS Thesis*, University of Arizona, Tucson.

Lal, D. and B. Peters. 1967. Cosmic Ray Produced Radioactivity on Earth. *Encyclopedia of Physics*, S. Fluegge, ed., Vol 46/2, *Cosmic Rays II*, K. Sitte, ed., Springer, Berlin, pp 551-612.

Lal, D. 1991. Cosmic Ray Labeling of Erosion Surfaces: In situ Production Rates and Erosion Models. *Earth and Planetary Science Letters*. 104:424-439

Mabbutt, J. A. 1977. *Desert Landforms*. MIT Press, Cambridge, Massachusetts

Nishiizumi, K., C. P. Kohl, J. R. Arnold, J. Klein, D. Fink, and R. Middleton. 1991. Cosmic Ray Produced ^{10}Be and ^{26}Al in Anarctic Rocks: Exposure and Erosion History. *Earth and Planetary Science Letters* 104:440-454

O'Brien, K, H. A. Sandmeier, G.E. Hansen, and J. E. Campbell. 1978. Cosmic Ray Induced Neutron Background Sources and Fluxes for Geometries of Air Over Water, Ground, Iron, and Aluminum. *Journal of Geophysical Research*. 83:114-120.

Pavich, M. J., L. Brown, J. Harden, J. Klein, and R. Middleton. 1986. ^{10}Be distribution in Soils from Merced River Terrace, California. *Geochimica et Cosmochimica Acta*. 50:1727-1735

Rama and M. Honda. 1961. Cosmic-Ray-Induced Radioactivity in Terrestrial Materials. *Journal of Geophysical Research*. 66 (10):3533-3539

Simpson, D.T. 1991. Soils and Geomorphology of the Quaternary Alluvial Sequence on the Western Piedmont of the Ajo Mountains, Organ Pipe Cactus National Monument, Pima County, Arizona. MS Thesis. University of New Mexico, Albuquerque

Wolfendale, A. W. 1963. *Cosmic Rays*. Philosophical Library Inc., New York

Yamashita, M., L. D. Stephens, and H. W. Patterson. 1966. Cosmic-Ray-Produced Neutrons at Ground Level: Neutron Production Rate and Flux Distribution. *Journal of Geophysical Research*. 71:3817-3834

Zreda, M. G., F. M. Phillips, D. Elmore, P. W. Kubik, P. Sharma, and R. I. Dorn. 1991. Cosmogenic Chlorine-36 Production Rates in Terrestrial Rocks. *Earth and Planetary Science Letters*. 105:94-109

Appendix

Chemical Compositions of Boulders on Qfc, Debris Flow, and Bedrock

Sample #	OP392-5	OP392-12	OP392-13	OP1092-1	OP1092-2	OP392-10
Rock Type	Trachyte	Trachy-andesite	Trachy-andesite	Trachy-andesite	Trachy-andesite	Trachy-andesite
Ref. #	2	11	11	11	11	12
Compound	% Weight of Rock					
SiO_2	67.9	58.8	56.40	58.80	58.80	54.50
TiO_2	.36	1.23	1.39	1.62	1.54	1.80
Al_2O_3	14.4	17.2	17.90	18.40	18.60	15.90
Fe_2O_3	2.48	5.94	6.65	6.70	6.29	8.78
MnO	.07	.08	0.16	0.10	0.10	0.14
MgO	.56	1.27	1.18	0.67	1.09	2.70
CaO	1.43	4.75	4.29	3.93	4.19	4.81
Na_2O	4.63	3.93	3.95	4.28	4.30	3.42
K_2O	4.32	3.85	3.72	3.82	3.59	3.33
P_2O_5	.08	0.42	0.54	0.07	0.07	0.49
%LOI	2.8	2.45	2.0	1.10	0.85	3.00
Total	99.3	100.30	98.20	99.50	99.40	99.20
Element	ppm in Rock					
Cl	36.3	38.6	46.3	54.7	65.6	49.4
B	5.6	12.2	13.3	13.3	11.5	7.9
Gd	4.7	8.8	12.0	5.8	5.8	8.8

*Note- Ref. # refers to the sample site number marked on the map in figure 2.

Chemical Compositions of Boulders on Qf1

Sample #	OP90-1	OP90- 2	OP90-3	OP90-5	OP90-11	OP90-12	OP90-13	OP91-6	OP91-7
Rock Type	Rhyolite	Rhyolite	Rhyolite	Trachyte	Rhyolite	Trachyte	Trachy-andesite	Trachyte	Rhyolite
Ref. #	1	1	1	1	3	3	3	6	6
Com-pound	% Weight of Rock								
SiO_2	72.51	69.21	75.87	59.18	74.09	64.30	62.07	64.05	70.02
TiO_2	0.27	0.36	0.14	1.54	0.13	0.93	0.72	0.94	0.20
Al_2O_3	13.21	14.58	12.67	15.38	11.08	16.06	15.24	16.12	12.62
Fe_2O_3	2.23	2.69	1.65	7.45	1.46	5.70	4.38	5.69	1.99
MnO	0.05	0.06	.04	0.12	0.05	0.07	0.05	0.10	0.06
MgO	0.58	0.71	0.46	1.91	1.12	1.49	1.71	2.38	1.26
CaO	2.21	1.56	1.23	3.18	2.19	3.40	2.76	3.29	3.68
Na_2O	5.73	4.05	3.11	6.39	2.66	4.35	3.85	4.20	3.57
K_2O	2.03	4.28	5.31	4.63	5.27	3.60	3.60	3.48	4.55
P_2O_5	0.06	0.07	0.05	0.35	0.08	0.23	0.15	0.31	.16
%LOI	5.12	3.11	1.30	1.57	3.01	1.49	2.22	1.95	3.67
Total	103.92	100.67	101.82	102.01	101.14	101.63	96.74	102.50	101.8
Element	ppm in Rock								
Cl	57.4	122.6	55.5	53.1	35.7	110.	55.1	71.6	36.5
B	22	14.0	6.0	20.0	19.0	8.6	7.1	8.4	9.6
Gd	3.1	4.9	3.8	10.0	3.4	5.9	7.1	7.3	3.9

Chemical Compositions of Boulders on Qt2

Sample #	OP90-7	OP90-8	OP90-9	OP90-10	OP91-3	OP91-4	OP91-5
Rock Type	Trachy-andesite	Rhyolite	Trachy-andesite	Rhyolite	Trachyte	Trachy-andesite	Rhyolite
Ref. #	2	2	2	2	5	5	5
Com-pound	% Weight of Rock						
SiO_2	58.50	72.58	57.96	77.66	63.50	59.93	73.33
TiO_2	1.41	0.30	1.55	0.27	0.93	1.60	0.23
Al_2O_3	18.04	14.63	16.99	13.01	16.17	16.20	13.93
Fe_2O_3	7.10	2.70	7.91	2.12	5.54	8.25	2.13
MnO	0.09	0.06	0.10	0.05	0.10	0.11	0.05
MgO	2.23	0.56	2.19	0.85	1.37	1.66	0.57
CaO	3.99	1.37	4.29	1.08	2.70	3.09	1.05
Na_2O	4.09	4.41	4.02	3.18	3.96	4.30	3.73
K_2O	4.12	4.71	4.18	4.72	3.66	4.51	5.00
P_2O_5	0.32	0.06	0.31	0.06	0.24	0.51	0.07
%LOI	1.86	1.22	1.44	0.97	2.63	1.73	1.24
Total	101.74	102.58	100.93	103.97	100.78	101.88	101.33
Element	ppm in Rock						
Cl	44.6	33.4	58.8	50.2	121.0	72.8	341.0
B	13.0	12.0	15.0	3.4	11.0	20.0	12.0
Gd	7.5	3.2	8.6	3.50	4.7	10.9	4.2

Chemical Compositions of Boulders on Qt1 and Qf2

Sample #	OP392-2	OP392-3	OP1092-5	OP91-1	OP91-2	OP392-4	OP1092-3
Rock Type	Trachyte	Trachyte	Trachyte	Rhyolite	Trachyte	Trachy-andesite	Rhyolite
Surface	Qt1	Qt1	Qt1	Qf2	Qf2	Qf2	Qf2
Ref. #	9	9	2	4	4	10	13
Compound	% Weight of Rock						
SiO_2	63.40	66.30	62.60	75.49	63.27	57.80	75.90
TiO_2	0.80	0.70	1.01	0.13	0.93	1.52	0.14
Al_2O_3	15.60	15.30	15.80	11.84	16.09	15.90	11.40
Fe_2O_3	4.25	3.68	5.09	1.82	5.70	7.64	1.17
MnO	0.07	0.06	0.09	0.09	0.08	0.18	0.05
MgO	1.18	0.74	1.22	1.22	2.62	1.30	0.22
CaO	3.56	2.41	3.21	1.62	3.72	3.80	0.79
Na_2O	4.10	4.20	4.31	2.38	4.26	3.80	2.70
K_2O	3.29	4.18	3.37	6.23	3.35	4.21	4.51
P_2O_5	0.24	0.17	0.09	0.19	0.29	0.72	0.04
%LOI	1.80	1.85	1.10	2.16	1.88	1.60	1.25
Total	98.60	99.90	97.90	103.16	102.19	98.50	98.20
Element	ppm in Rock						
Cl	94.1	79.1	49.8	59.6	86.4	63.9	36.8
B	8.0	10.7	3.0	10.0	7.6	22.3	2.9
Gd	6.0	5.2	1.9	3.7	5.4	13.3	4.9